Amino-Functionalized Polystyrene Nanoparticles Activate the NLRP3 Inflammasome in Human Macrophages

Oleg Lunov,[†] Tatiana Syrovets,[†] Cornelia Loos,[†] G. Ulrich Nienhaus,[‡,§] Volker Mailänder,[⊥,∥] Katharina Landfester,[⊥] Mustapha Rouis,[#] and Thomas Simmet[†,*]

[†]Institute of Pharmacology of Natural Products & Clinical Pharmacology, Ulm University, Ulm, Germany, [‡]Institute of Applied Physics and Center for Functional Nanostructures (CFN), Karlsruhe Institute of Technology (KIT), Karlsruhe, Germany, [§]Department of Physics, University of Illinois at Urbana—Champaign, Illinois 61801, United States, [⊥]Max Planck Institute for Polymer Research, Mainz, Germany, [∥]3rd Department of Medicine, University Medical Center, Mainz, Germany, and [#]Unité de Recherche, UR-04, Vieillissement, Stress et Inflammation, Université Pierre et Marie Curie, Paris, France

ABSTRACT Specifically designed and functionalized nanoparticles hold great promise for biomedical applications. Yet, the applicability of nanoparticles is critically predetermined by their surface functionalization. Here we demonstrate that amino-functionalized polystyrene nanoparticles (PS-NH_2) of ~100 nm in diameter, but not carboxyl- or nonfunctionalized particles, trigger NLRP3 inflammasome activation and subsequent release of proinflammatory interleukin 1β (IL-1β) by human macrophages. PS-NH_2 induced time-dependent proton accumulation in lysosomes associated with lysosomal destabilization, release of cathepsin B, and damage of the mitochondrial membrane. Accumulation of mitochondrial reactive oxygen species was accompanied by oxidation of thioredoxin, a protein playing a central role in maintaining the cellular redox balance. Upon oxidation, thioredoxin dissociated from the thioredoxin-interacting protein (TXNIP). Liberated TXNIP, in turn, interacted with the NLRP3 protein, resulting in a conformational change of the pyrin domain of the NLRP3 protein, as was predicted by molecular modeling. Consequently, this prompted assembly of the NLRP3 inflammasome complex with recruitment and activation of caspase-1, inducing IL-1β release by cleavage of pro-IL-1β. The central role of the NLRP3 inflammasome for cytokine production was confirmed by *in vitro* knockdown of NLRP3 and of the adaptor protein ASC, confirming that other inflammasomes were not activated by PS-NH_2. The PS-NH_2-mediated proinflammatory macrophage activation could be antagonized by the radical scavenger *N*-acetyl-L-cysteine, which prevented mitochondrial damage, caspase-1 activation, and the subsequent release of IL-1β. Our study reveals the molecular mechanism of NLRP3 inflammasome activation by amino-functionalized nanoparticles and suggests a strategy as to how such adverse effects could be antagonized.

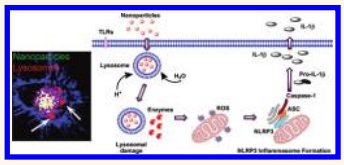

KEYWORDS: macrophages · polystyrene particles · inflammasome · interleukin-1β · thioredoxin · reactive oxygen species

Nanomaterials are gaining steadily increasing attention in almost all fields of research and technology. Their importance is mainly based on their highly specialized functionality that is determined not only by properties of the bulk materials but also by size, form, surface area, and specific surface properties and characteristics of such particles.[1−3] Nanoparticles are widely employed in catalytic and separation processes, and they are already well established in a variety of biological and medical applications. Notwithstanding, they are still expected to enable major breakthroughs in biomedical applications, for example, in targeted drug delivery. Nanoparticles are already indispensable in magnetic resonance imaging, where they increase soft tissue contrast. They are further used in hyperthermia treatment, in gene delivery, in studies of cell mechanics, as fluorescent biological labels, and for the separation and purification of biological molecules and cells.[1,2] In biological systems, nanosized particles may play a dual role. On one hand, they may elicit toxic effects,[4] whereas, on the other hand, novel nanoscale diagnostic and drug-delivery vehicles hold great promise for better medical treatment.[5] It is obvious that, especially for therapeutic purposes, adverse effects should be minimized to warrant safe applications. Studies dealing specifically with the long-term toxicity of nanoparticles have appeared only recently, and they are still comparatively few in number.[6−8]

Polystyrene nanoparticles possess many advantages, including straightforward synthesis in a wide range of sizes, relatively low costs, easy separation, and easy surface modification. These properties facilitated their application as biosensors,[9] in photonics,[10] and in self-assembling nanostructures.[11] Surface modification, high loading capacity, and colloidal stability in biological media render them a perfect platform for studying the biomedical consequences of various surface modifications.[12] We used those properties to study the effects of surface functionality on the nanoparticle cell interaction. A detailed understanding of the impact of the surface

* Address correspondence to thomas.simmet@uni-ulm.de.

Received for review August 14, 2011 and accepted November 23, 2011.

Published online November 23, 2011
10.1021/nn203596e

functionalization is a prerequisite for the rational design of nanomaterials targeting distinct cell types for diagnostic or therapeutic purposes.

Macrophages are critical regulators of local homeostasis. They are highly adaptive components of the innate immune system and respond in diverse ways to different pathogens.[13,14] Macrophages are causally involved in all types of chronic inflammatory diseases including atherosclerosis, rheumatoid arthritis, and neuroinflammatory diseases, where they play a crucial role in the initiation and maintenance of the inflammatory process that ultimately leads to tissue damage and destruction.[15,16] Indeed, macrophages are multifunctional phagocytic cells distributed throughout the body. They are fully equipped to sense and internalize endogenous and exogenous materials, such as viruses, microorganisms, cells, cell debris, and foreign particulate matter including a variety of engineered nanoparticles.[15,17,18] Unwanted interactions between diagnostic or therapeutic nanomaterials and macrophages of the reticuloendothelial system stress the significance of thorough studies of the characteristics and structural determinants of nanoparticles that govern their interactions with cells.

Inflammation is generally a key factor in the development of a variety of diseases.[19,20] Cytokines of the interleukin-1 family are prime mediators of innate immunity and inflammation. Particularly, interleukin-1β (IL-1β) is involved in the initiation and propagation of acute and chronic inflammatory processes. Macrophages are the most important source of IL-1β,[21] which is processed from its biologically inactive precursor pro-IL-1β by caspase-1 of the NLRP3 inflammasome complex.[21,22] The mechanisms of NLRP3 activation are only poorly understood. Hence, the analysis of the NLRP3 inflammasome activation is of great interest.[23−25] Recently, it has been demonstrated that certain nanoparticles, as well as uric acid crystals that trigger gout, induce inflammation associated with the activation of multiprotein inflammasome complexes.[23,26−31]

Previously we found that amino-functionalized polystyrene nanoparticles preferentially target treatment-resistant prostate cancer cells.[32] However, by an unknown mechanism, polystyrene nano- but not microparticles also seem to induce pulmonary inflammation.[8,33] Taking into account the significance of particle surface functionalization for targeted biomedical application, it is of great importance to study the key determinants governing the reciprocal interaction between nanomaterials and the surface of biological membranes. Thus, aiming to engineer particles with particular therapeutic properties that additionally target distinct cell types, it is crucial to understand how distinct chemical surface modifications will affect biological responses. In the present study, we have investigated the long-term effects of functionalized and nonfunctionalized polystyrene nanoparticles on physiological functions of human macrophages, as relevant cells of the innate immune system.

RESULTS AND DISCUSSION

Synthesis of Polystyrene Nanoparticles and Their Physicochemical Characterization. Amino- (PS-NH_2), carboxyl- (PS-COOH), or nonfunctionalized (PS) polystyrene nanoparticles were synthesized by the miniemulsion process.[34,35] The physicochemical properties of the nanoparticles were characterized by dynamic light scattering, UV/vis absorption spectroscopy, and other techniques and are summarized in Table S1, Supporting Information. All three types of particles had similar mean hydrodynamic diameters of about 110 nm. The highly negative or positive zeta potentials reflected the functionalization of the particles with either carboxyl or amino groups, respectively. The particles had approximately the same surface density of charged groups and contained basically the same amount of the fluorescent dye PMI, which was incorporated stably into the particles during their synthesis (Table S1). Previously, we analyzed the mechanisms of nanoparticle uptake by human monocyte-derived macrophages.[32] In the present study, we investigated the long-term effects of functionalized polystyrene nanoparticles on human macrophages.

Prolonged Treatment of Human Macrophages with PS-NH_2 Nanoparticles Induces Lysosomal Permeabilization. It has previously been noticed that nanoparticle characteristics, such as particle size and surface properties, are important determinants of cellular responses, including pathological alterations.[30,32,36]

Exposure of a murine macrophage cell line to the amino-functionalized nanoparticles induced cell death. It was hypothesized that the cytotoxic effect of the nanoparticles might involve rupture of lysosomes.[37] To determine whether the polystyrene nanoparticles might induce lysosomal destabilization, the subcellular distribution of the nanoparticles in human macrophages and the lysosomal integrity were analyzed by confocal microscopy (Figure 1A and Figure S1A, Supporting Information). DQ ovalbumin, a self-quenched conjugate of ovalbumin that exhibits bright fluorescence upon proteolytic degradation, was used to stain the lysosomes in living cells. In controls and cells treated with PS-COOH or PS nanoparticles, DQ ovalbumin was localized in small lysosomes. In contrast, macrophages treated with PS-NH_2 contained large swollen lysosomes, indicating lysosomal destabilization, which could be accompanied by leakage of proteolytic lysosomal enzymes into the cytosol (Figure 1A and Figure S1A, Supporting Information).

To address the possible lysosomal leakage induced by amino-functionalized polystyrene nanoparticles, we used the lysosomotropic dye acridine orange (AO). AO uptake in lysosomes leads to red fluorescence, which decreases when the dye is leaking from this compartment into the cytosol. After treatment with nanoparticles, the

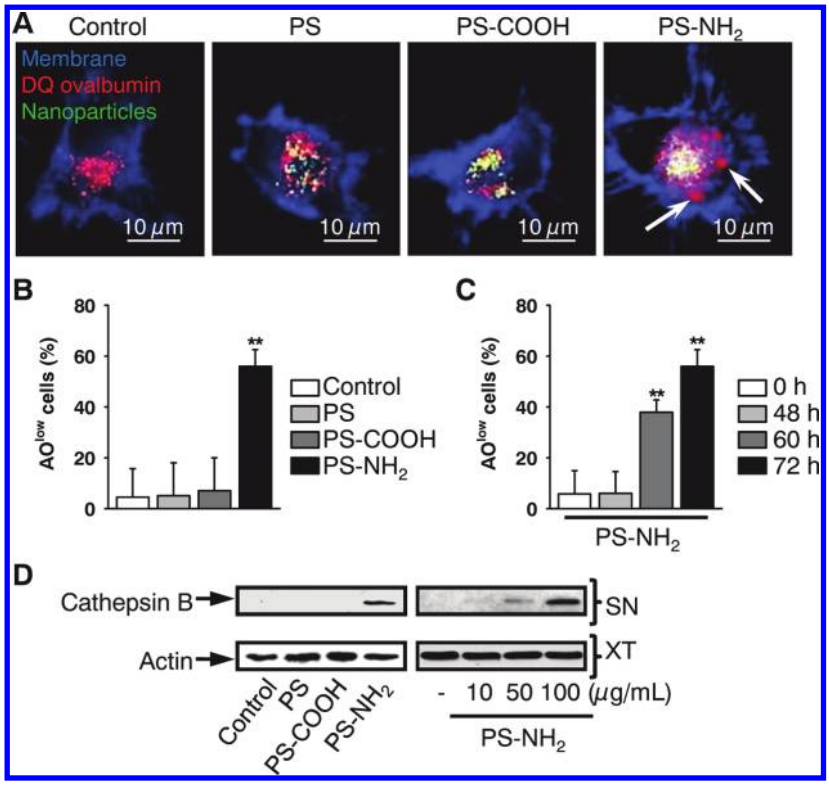

Figure 1. $PS\text{-}NH_2$ nanoparticles induce lysosomal rupture in human macrophages. (A) Functionalized and nonfunctionalized polystyrene nanoparticles co-localize with the lysosomal compartment. Spinning disk confocal microscopy of human macrophages incubated with different types of polystyrene nanoparticles (100 μg/mL, green) for 72 h and stained for 60 min with DQ ovalbumin (10 μg/mL, red). Cell membranes were stained with CellMask Deep Red (blue); original magnifications were 640×. (B) $PS\text{-}NH_2$ nanoparticles induce lysosomal leakage. Macrophages were treated with polystyrene nanoparticles (100 μg/mL) for 72 h, stained with acridine orange (AO), and analyzed by flow cytometry to detect the population of AO^{low} cells exhibiting leaking lysosomes; $^{**}p < 0.01$ *vs* control, mean ± SEM, $n = 3$. (C) Time-dependence of lysosomal permeabilization. Macrophages were treated with $PS\text{-}NH_2$ nanoparticles (100 μg/mL) for different periods of time and analyzed by flow cytometry as in (B); $^{**}p < 0.01$ *vs* control, mean ± SEM, $n = 3$. (D) Immunoblot analysis of active cathepsin B in the cytosol of macrophages stimulated with different polystyrene nanoparticles (100 μg/mL) or treated with different concentrations of $PS\text{-}NH_2$ nanoparticles for 72 h. Data are presented as mean ± SEM from at least three independent experiments. Macrophages were primed for 3 h with 10 ng/mL LPS.

cells were stained with AO and analyzed by flow cytometry. M1-gating was used to assess the percentage of AO^{low} cells (Figure S1B, Supporting Information), which represents the cells with permeable, leaky lysosomes. Treatment with $PS\text{-}NH_2$, but not PS-COOH or nonfunctionalized PS nanoparticles, induced a significant increase in the percentage of AO^{low} macrophages (Figure 1B). The lysosomal permeabilization induced by $PS\text{-}NH_2$ was delayed in time (Figure 1C). Consistent with our previous findings,[32] $PS\text{-}NH_2$ did not induce lysosomal leakage within the first 48 h. However, in line with the destabilization of the lysosomes by the $PS\text{-}NH_2$ nanoparticles after three days of exposure, release of mature lysosomal cathepsin B into the cytosol of the macrophages became detectable as well (Figure 1D).

The differing biological effects of $PS\text{-}NH_2$ compared to PS and PS-COOH nanoparticles cannot be explained by a more efficient uptake of $PS\text{-}NH_2$ by macrophages. In fact, $PS\text{-}NH_2$ were taken up by cells less efficiently than PS and PS-COOH (Figure S2, Supporting Information). We hypothesized that $PS\text{-}NH_2$ might induce lysosomal damage due to the so-called ``proton sponge'' effect.[38] The postulated mechanism of the "proton sponge effect" involves sequestration of protons by the amines on the particle surface, thereby keeping the proton pump working, which leads to the retention of one Cl^- ion and one water molecule for each proton that enters the lysosome. Of course, this process would then lead to lysosomal swelling and finally to osmotic rupture.[38] To address the potential role of the "proton sponge effect" in the $PS\text{-}NH_2$ nanoparticle-induced lysosomal leakage, we determined the lysosomal pH using the pH-sensitive marker LysoSensor (Figure 2). Consistent with the hypothesis, macrophage treatment with $PS\text{-}NH_2$ nanoparticles led to acidification of the lysosomal compartment of the cells, confirming that $PS\text{-}NH_2$ nanoparticles activate the lysosomal proton pump. By the aforementioned mechanism, this process will finally result in lysosomal swelling and leakage of lysosomal enzymes, such as cathepsin B.

Lysosomal Permeabilization Induced by $PS\text{-}NH_2$ Nanoparticles Causes Mitochondrial Dysfunction. When cathepsin B comes in contact with mitochondrial membranes, it

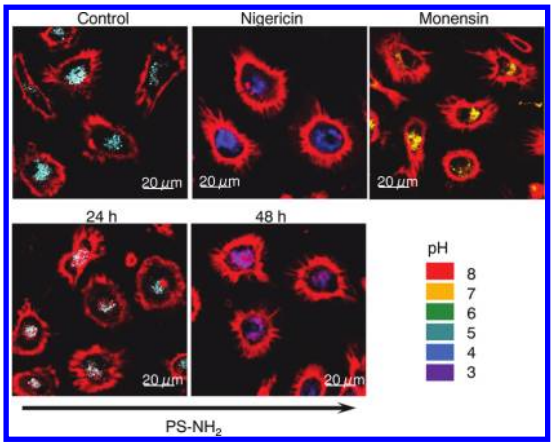

Figure 2. PS-NH_2 nanoparticles induce acidification of lysosomes in human macrophages. Confocal microscopy of human macrophages incubated with PS-NH_2 nanoparticles (100 μg/mL) for the indicated periods of time. Lysosomal pH was measured using LysoSensor Yellow/Blue DND-160 (Invitrogen) at 450 $\pm$ 40 and 510 $\pm$ 30 nm, both excited with a 405 nm laser. Cell membranes were stained with CellMask Deep Red (blue). Pseudocolored images are shown. Nigericin (20 μM, 20 min) and monensin (20 μM, 30 min) were used as calibration controls for pH 4.5 and 7.6, respectively; original magnifications were 640×.

causes mitochondrial dysfunction.[39,40] To investigate whether polystyrene particles can perturb mitochondrial function, we used the fluorescent dye JC-1. JC-1 is a cationic dye that exhibits a potential-dependent accumulation in mitochondria, which can be monitored by a fluorescence emission shift from green to red using flow cytometry. As expected, PS-NH_2 induced depolarization of the mitochondrial membrane, as indicated by a decrease of the red-to-green fluorescence intensity ratio (Figure S3, Supporting Information). In contrast, PS and PS-COOH nanoparticles did not induce any significant changes in the mitochondrial membrane potential when compared to controls (Figure 3A and Figure S3, Supporting Information). Apart from mitochondrial depolarization, PS-NH_2 nanoparticles also induced cytochrome *c* release (Figure S4, Supporting Information), clearly demonstrating that PS-NH_2 nanoparticles induce mitochondrial dysfunction including leakage. It has been shown that lysosomal rupture and the associated release of lysosomal enzymes promote the mitochondrial production of oxidants.[41,42] Therefore, we investigated the putative, nanoparticle-mediated, mitochondrial generation of reactive oxygen species (ROS) with the fluorescent indicator dye MitoSOX Red (Figure 3B). Indeed, exposure of macrophages to PS-NH_2 led to significant mitochondrial ROS production (Figure 3B), whereas PS and PS-COOH nanoparticles did not induce any ROS. The PS-NH_2-induced mitochondrial ROS production showed a considerable time delay. In analogy to the time dependence of lysosomal rupture, the mitochondrial ROS production was observed to increase not earlier than 60 h after exposure to PS-NH_2 (Figure S5A,B, Supporting Information).

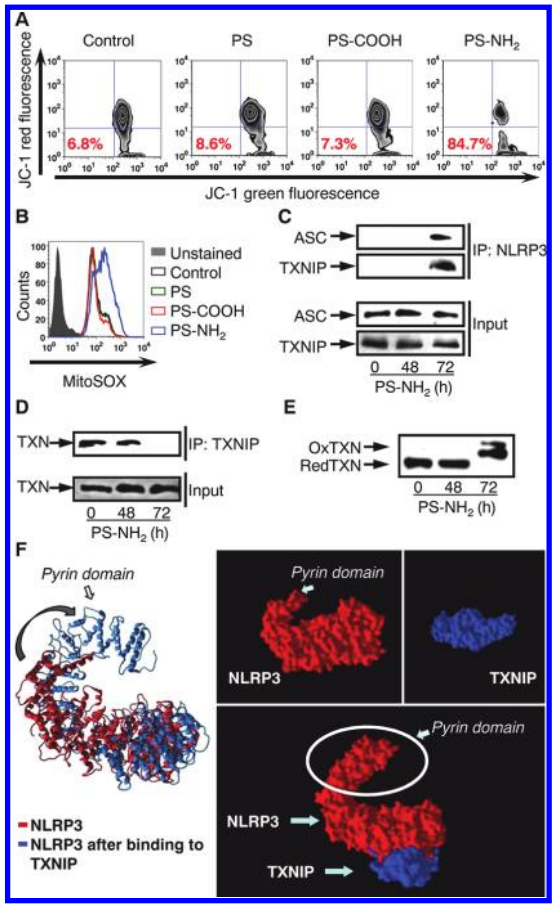

Figure 3. PS-NH_2 nanoparticles induce mitochondrial dysfunction in human macrophages. (A) After priming with LPS, macrophages were stimulated with different polystyrene nanoparticles (100 μg/mL) for 72 h, stained with 2 μM JC-1 for 30 min, and analyzed by flow cytometry. Numbers show amounts of JC-1 red^{low} cells exhibiting damaged mitochondria. (B) Cells were treated as in (A), stained with redox-sensitive dye MitoSOX (5 μM) for 10 min, and analyzed by flow cytometry. Filled gray peak, unstained control; black peak, control; green peak, PS; red peak, PS-COOH; blue peak, PS-NH_2. (C) Immunoprecipitation and immunoblot analysis of the interaction of TXNIP with NLRP3 in macrophages treated with PS-NH_2 (100 μg/mL) for different periods as indicated. (D) Dissociation of TXNIP-TXN complex upon PS-NH_2 (100 μg/mL) stimulation, as revealed by immunoprecipitation. IP, immunoprecipitation; input ensures equal loading. (E) PS-NH_2 nanoparticles induce TXN oxidation in macrophages. Cells were stimulated with PS-NH_2 (100 μg/mL) for the indicated periods of time, and the redox status of TXN was analyzed by redox Western blot. Data are representative of at least three independent experiments. (F) Binding of TXNIP induces exposure of the pyrin domain of NLRP3 inflammasome, as predicted by molecular modeling. Modeling was performed using Hex 6.3 software. NLRP3, NLR family, pyrin domain-containing 3 inflammasome; TXN, thioredoxin; TXNIP, thioredoxin-interacting protein; ASC, apoptosis-associated speck-like protein; CARD, caspase activation and recruitment domain; LRR, leucine-rich repeat.

ROS Accumulation Triggers Assembly of the NLRP3 Inflammasome. ROS are emerging as key effectors in signal transduction.[43] Indeed, high levels of ROS may induce intracellular signals, but can also damage cellular structures, finally leading to cell death.[44] Moreover,

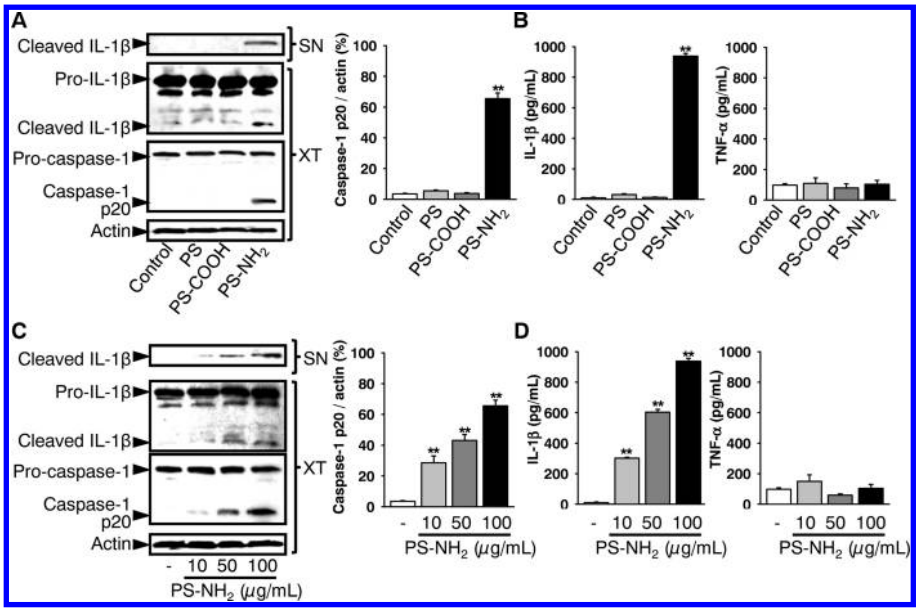

Figure 4. PS-NH_2 nanoparticles activate the NLRP3 inflammasome and induce release of IL-1β but not of TNF-α by human macrophages. (A) Macrophages were stimulated with different polystyrene nanoparticles (100 μg/mL) for 72 h. Caspase-1 and IL-1β cleavage and IL-1β release into the supernatant were analyzed by Western immunoblot. The graph shows the densitometric analysis of caspase-1 activation. (B) Cells were treated as in (A); IL-1β and TNF-α secretion was detected by ELISA. **$p < 0.01$ *vs* control, mean $\pm$ SEM, $n = 3$. (C) Macrophages were stimulated with different concentrations of PS-NH_2 nanoparticles for 72 h and analyzed by Western immunoblot. The graph shows the densitometric analysis of the immunoblot. (D) Cells were treated as in (C); IL-1β and TNF-α secretion was detected by ELISA. Data are presented as mean $\pm$ SEM from at least three independent experiments, **$p < 0.01$ *vs* control. Macrophages were primed for 3 h with 10 ng/mL LPS. Actin was the loading control.

accumulation of damaged, ROS-producing mitochondria may elicit NLRP3 inflammasome activation.[45] We, therefore, hypothesized that the accumulation of ROS might trigger assembly of the NLRP3 inflammasome in macrophages.

Inflammasomes are cytosolic molecular complexes that, upon activation, exhibit enzymatic activity mediated by caspase-1.[22] Pathogens, stress, or danger signals are activators of inflammasomes, which lead finally to cleavage and release of cytokines such as mature IL-1β. The most studied inflammasome is the one containing a nucleotide-binding oligomerization domain-like receptor protein, NOD-like receptor family, pyrin domain containing 3 (NLRP3).[46] Upon activation, NLRP3 recruits an adaptor protein, ASC, containing a C-terminal caspase activation and recruitment domain (CARD) and a protease, caspase-1, to form the NLRP3 inflammasome. To investigate whether PS-NH_2 treatment leads to NLRP3 inflammasome formation, we immunoprecipitated NLRP3 to analyze the proteins within the NLRP3 complex. The ASC protein was indeed precipitated together with NLRP3 upon PS-NH_2 stimulation. Again, interaction of ASC with NLRP3 was delayed and could be observed not earlier than 72 h after stimulation of macrophages with PS-NH_2 (Figure 3C). This observation is in line with our findings that the PS-NH_2-induced lysosomal destabilization and mitochondrial ROS production were delayed by a similar time interval.

Recently, thioredoxin-interacting protein (TXNIP) has been identified as a NLRP3 binding partner, which, under conditions of oxidative stress, binds to NLRP3 and leads to its activation.[47] Consistent with this finding, we observed that PS-NH_2 stimulation for 72 h led to formation of TXNIP–NLRP3 complexes that could be identified by immunoprecipitation (Figure 3C).

TXNIP is a physiological inhibitor of thioredoxin (TXN) redox activity.[48] TXN is a small (12 kDa) protein with a conserved active site containing the pentapeptide Trp-Cys-Gly-Pro-Cys, which plays an important defensive role against oxidative stress by scavenging ROS. Binding of ROS leads to TXN oxidation.[49] TXNIP interacts directly with the redox-active domain of TXN and presumably functions as a negative regulator of TRX.[48] We observed that TXNIP dissociates from TXN upon PS-NH_2 treatment (Figure 3D). This dissociation event correlated with ROS production (Figure 3B and Figure S5A,B, Supporting Information). Consistent with the PS-NH_2-mediated ROS production, such a treatment also led to oxidation of TXN (Figure 3E). All these processes, ROS increase, TXN oxidation, TXN-TXNIP dissociation, and TXNIP-NLRP3 association, occurred with a time delay of 72 h following addition of PS-NH_2.

In silico molecular modeling of the TXNIP–NLRP3 interaction revealed that NLRP3 interacts with TXNIP *via* leucine-rich repeat (LRR) and NACHT domains (Figure 3F), consistent with the results by Zhou *et al.*[47] Computational docking and scoring studies using Hex 6.3[50,51] revealed conformational changes in the pyrin domain of NLRP3 that were induced by TXNIP binding (Figure 3F). The pyrin domain has been shown to

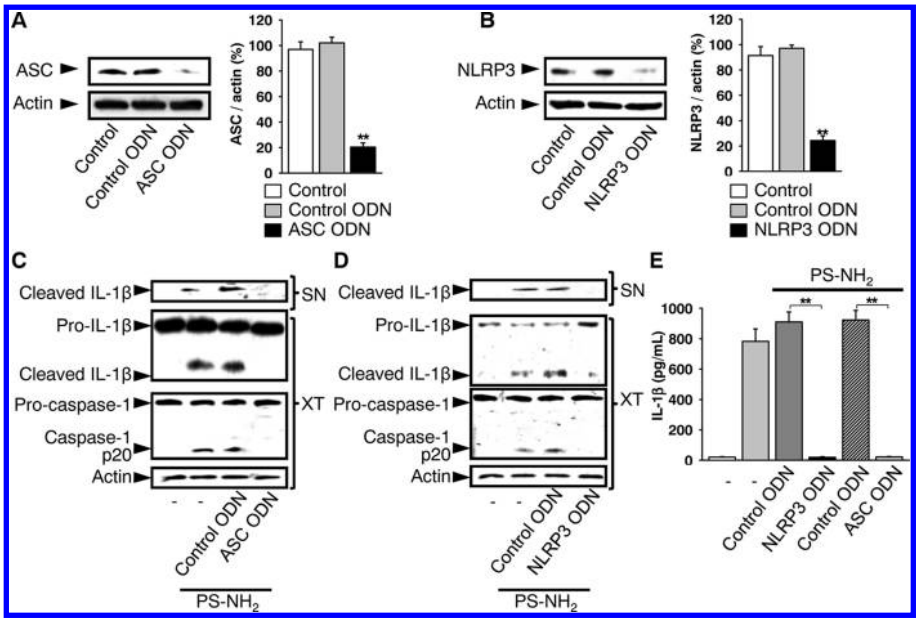

Figure 5. Downregulation of ASC and NLRP3 impairs NLRP3 inflammasome activation and IL-1β release induced by PS-NH_2 nanoparticles. (A) Antisense ODN downregulate the expression of ASC in human macrophages. After treatment with ODN against ASC or control sequence for 24 h, ASC expression was detected by immunoblotting. The graph shows the densitometric analysis of the immunoblots. **$p < 0.01$ *vs* control, mean $\pm$ SEM, $n = 3$. (B) Antisense ODN downregulate the expression of NLRP3 in human macrophages. After treatment with ODN against NLRP3 or control sequence for 24 h, NLRP3 expression was detected by immunoblotting. The graph shows the densitometric analysis of the immunoblots. **$p < 0.01$ *vs* control, mean $\pm$ SEM, $n = 3$. Treatment with antisense ODN against ASC (C) or NRLP3 (D) impairs inflammasome activation induced by PS-NH_2 nanoparticles. Macrophages were treated with the corresponding ODN for 24 h; then PS-NH_2 nanoparticles (100 μg/mL) were added for an additional period of 72 h, and the cells and supernatants were analyzed by Western immunoblot. (E) Macrophages were treated with antisense ODN against ASC or NRLP3, then stimulated with PS-NH_2 nanoparticles (100 μg/mL) for 72 h, and the IL-1β secretion was detected by ELISA. Data are presented as mean $\pm$ SEM from at least three independent experiments, **$p < 0.01$ *vs* control. Macrophages were primed for 3 h with 10 ng/mL LPS. Actin was the loading control.

sequester ASC, thereby promoting binding of caspase-1 to the CARD domain within ASC, followed by caspase-1 activation.[22] Therefore, a conformational change in the pyrin domain, which might become more accessible for the interaction with ASC upon binding to TXNIP, could presumably trigger the NLRP3 inflammasome activation.

PS-NH_2 Nanoparticles Activate the NLRP3 Inflammasome and Induce IL-1β Secretion in Human Primary Macrophages. Activation of the inflammasome triggers cleavage and activation of caspase-1 and release of active IL-1β, which promotes inflammatory responses.[52] PS-NH_2 but not PS or PS-COOH nanoparticles induced caspase-1 and IL-1β cleavage and IL-1β secretion (Figure 4A,B). Moreover, PS-NH_2 induced a concentration-dependent caspase-1 activation and IL-1β secretion, which were already observed at concentrations as low as 10 μg/mL (Figure 4C,D). On the other hand, PS or PS-COOH nanoparticles induced neither cleavage of caspase-1 or IL-1β nor IL-1β secretion in the concentration range from 10 to 100 μg/mL (Figure S6A,B, Supporting Information). PS-NH_2 nanoparticles were potent stimuli for IL-1β secretion in human primary macrophages, whereas release of the inflammasome-independent cytokine TNF-α was not induced by PS-NH_2 nor by any other type of polystyrene nanoparticles tested (Figure 4B,D). Interestingly, PS-NH_2 particles activate the inflammasome also without LPS priming, though to a lesser extent (Figure S6C, Supporting Information).

Several inflammasomes, NLRP1, NLRP3, NLRC4, and AIM2, are presently known.[22] To enquire whether PS-NH_2 nanoparticles activate specifically NLRP3 but not the other inflammasomes, we knocked down the expression of NLRP3 and its adaptor protein ASC by specific phosphothioate-modified antisense oligodeoxynucleotides (ODN). As controls, we used the ODN containing the same set of nucleotides but in a scrambled order.[32,53] The ASC antisense ODN inhibited the ASC expression in macrophages by 79.7 $\pm$ 3.2% (Figure 5A). Antisense ODN against NLRP3 inhibited the expression of NLRP3 by 75.8 $\pm$ 3.8% (Figure 5B). In addition, both ASC and NLRP3 antisense ODNs impaired significantly the processing of caspase-1 (Figure 5C,D) and consequently reduced IL-1β cleavage and secretion by macrophages (Figure 5C–E), clearly confirming that the NLRP3 inflammasome specifically mediates the response to PS-NH_2 nanoparticles.

Scavenging of ROS Abolishes NLRP3 Inflammasome Activation Induced by PS-NH_2 Nanoparticles and Reduces the Secretion of IL-1β by Human Macrophages. The required presence of

ASC and NLRP3[22] for PS-NH_2-mediated IL-1β release confirmed that PS-NH_2 nanoparticles induce formation of the NLRP3 inflammasome. Generation of ROS has been shown to be crucial for the NLRP3 inflammasome activation. Therefore, ROS scavengers such as *N*-acetyl-L-cysteine (NAC) can block this activation.[19,54] To determine whether ROS scavenging would also suppress PS-NH_2-mediated NLRP3 inflammasome activation, macrophages were treated with PS-NH_2 nanoparticles for 72 h in the presence of 25 mM NAC. Indeed, NAC was able to antagonize the production of mitochondrial ROS elicited by PS-NH_2 in macrophages (Figure 6A). Moreover, NAC potently reduced caspase-1 cleavage as well as maturation and subsequent release of IL-1β (Figure 6B,C).

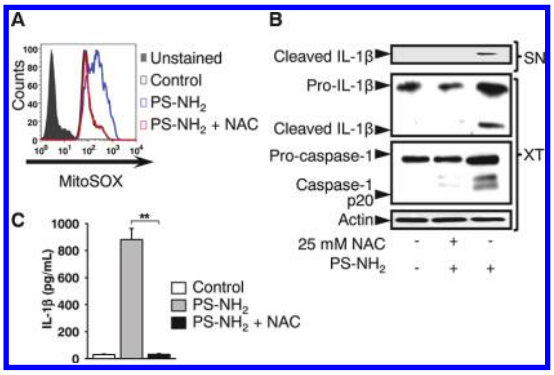

Figure 6. NLRP3 inflammasome activation induced by PS-NH_2 is mediated by mitochondrial ROS production. (A) Macrophages were stimulated with PS-NH_2 nanoparticles (100 μg/mL) for 72 h with or without 25 mM *N*-acetyl-L-cysteine (NAC), stained with 5 μM MitoSOX for 10 min and analyzed by flow cytometry. Filled gray peak, unstained control; black peak, control; blue peak, PS-NH_2; red peak, PS-NH_2 + 25 mM NAC. (B) Macrophages were stimulated with PS-NH_2 (100 μg/mL) for 72 h with or without 25 mM NAC and analyzed by Western immunoblot. (C) Cells were treated as in (B); IL-1β secretion was detected by ELISA. All data are presented as mean $\pm$ SEM from at least three independent experiments, **$p < 0.01$ *vs* control.

Three signaling pathways have been proposed to date leading to inflammasome activation. In the first model, an activator induces caspase-1 cleavage and activation *via* cryopyrin.[55] In the second model, cathepsin B released from ruptured lysosomes cleaves an unidentified substrate and triggers inflammasome activation.[21,25] In a third model, ROS generated by NLRP3 activators induce inflammasome activation.[19,22,47] Here, we propose an integrated model of NLRP3 activation induced by PS-NH_2 nanoparticles. In this model, both lysosomal rupture and generation of mitochondria-derived ROS are indispensible for the activation of NLRP3 by amino-functionalized nanoparticles (Figure 7, Figure S7, Supporting Information). This hypothesis is supported by data showing that knockdown of antioxidant TRX enhances IL-1β activation induced by silica, uric acid crystals, and asbestos.[56] Similarly, inhibition of ROS production macrophages has been shown to decrease inflammasome activation.[57]

CONCLUSION

Our study revealed that amino-functionalized, but not carboxyl- or nonfunctionalized polystyrene nanoparticles induce NLRP3 inflammasome activation and subsequent IL-1β production by human macrophages. The inflammasome activation was mediated by lysosomal rupture and leakage of active cathepsin B to the cytosol. These processes elicited mitochondrial damage and production of ROS. Accumulation of mitochondrial ROS led to oxidation of the redox-active TXN and its subsequent dissociation from TXNIP. Liberated TXNIP interacted with NLRP3 and triggered a conformational change of NLRP3 binding of the adaptor protein ASC, resulting in inflammasome activation

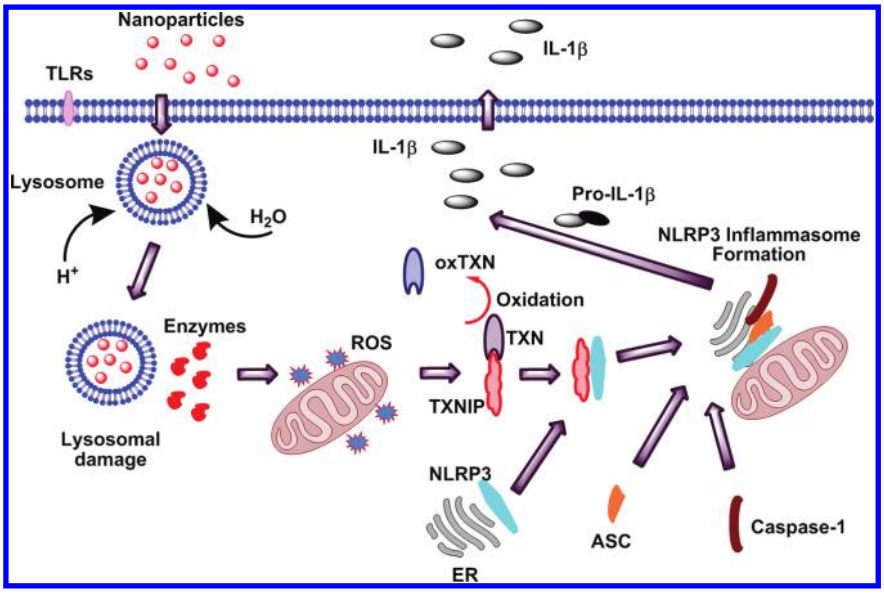

Figure 7. Scheme of NLRP3 inflammasome activation in macrophages after stimulation with PS-NH_2 nanoparticles.

and IL-1β production. Activation of the NLRP3 inflammasome could be blocked by a ROS scavenger. Thus, surface modification with amino groups turned biologically inert nanoparticles into potent activators of inflammatory responses. Hence, the effects of surface modification of particles require intensive studies, which should be considered when such particles are intended for use in biomedical applications.

MATERIALS AND METHODS

Preparation and Physicochemical Characterization of the Nanoparticles. Fluorescent nanoparticles were synthesized by the miniemulsion polymerization process.[34,35] Details of the synthesis of polystyrene nanoparticles have been described previously.[32] After synthesis, surfactant was removed by Amicon ultrafiltration (100 kDa), extensive dialysis, and washing. Before being used, the particle suspensions were dispersed by sonification, and the absence of agglomeration was controlled by a Zetasizer Nano (Malvern Instruments, UK). The average particle size, polydispersity index (PDI), and zeta potential were determined by dynamic light scattering (DLS) in 1 mM KCl solution at pH 7.0 using a Zetasizer Nano. Incorporated PMI was quantified by UV/vis absorption spectroscopy (Lambda 16, Perkin-Elmer, Rodgau, Germany) of dried nanoparticles dissolved in tetrahydrofuran. The surface charge density was determined by polyelectrolyte titration using a PCD 02 particle charge detector (Muetek, Germany) in combination with a 702 SM Titrino automatic titrator (Metrohm, Switzerland).[35] All three types of particles were stable in physiological media. Details on the synthesis, morphology, and stability of the used particles have been published previously.[34,35]

Cell Differentiation and Treatment. Macrophages were differentiated from human monocytes isolated from buffy coats by density gradient centrifugation using Histopaque 1077. To induce differentiation, the monocytes were treated every other day with 15 ng/mL M-CSF (R&D Systems); they were characterized by flow cytometry and used at day 7 for experiments with nanoparticles.[58] Macrophages (1×10^6 cells/mL RPMI 1640, 10% FCS) were primed for 3 h with 10 ng/mL LPS and then treated with the indicated concentrations of particles for different time periods.

Cellular Staining with Fluorescent Probes and Flow Cytometry. After treatment with nanoparticles, macrophages were stained with the fluorescent dyes diluted in HBSS for 15−30 min at 37 °C in the dark. The following dyes were used: 5 μg/mL acridine orange (AO), for assessment of lysosomal integrity;[8] 5 μM MitoSOX (Invitrogen), for detection of mitochondrial ROS; 2 μM JC-1 (Invitrogen), for determination of mitochondrial depolarization. Flow cytometry was performed using a FACScan (Becton Dickinson) and FlowJo software.

Confocal Microscopy. Macrophages seeded on IBIDI slides (Munich, Germany) were incubated with different types of polystyrene nanoparticles (100 μg/mL) for 72 h; DQ ovalbumin (10 μg/mL, Invitrogen) was added for 60 min. Cell membranes were stained with CellMask Deep Red (Invitrogen). Fluorescence images were taken with the acquisition software Andor iQ 1.6 using a custom-designed spinning disk confocal microscope consisting of a CSU10 scan head (Yokogawa, Tokyo, Japan), an inverted microscope (Axio Observer, Zeiss) with an oil immersion objective (UPlanSApo 60 × /1.35, Olympus), an environmental control (PECON, Erbach, Germany), an image splitting unit (OptoSplit II, Cairn Research, Faversham, UK), and an EMCCD camera (DV-887, Andor, Belfast, UK).[59,60] ImageJ software (NIH) was used for image processing.

Western Immunoblot Analysis. Supernatants (SN) were precipitated by methanol−chloroform precipitation. Aliquots of whole cell lysates (XT) and supernatants were separated by SDS-PAGE, transferred, and probed with specific antibodies against IL-1β (Cell Signaling), caspase-1 (Imgenex), NLRP3 (Epitomics), ASC, and cathepsin B (both from Santa Cruz) as described;[61,62] actin (Chemicon) staining served as loading control.

Knockdown of NLRP3 and ASC. For *in vitro* knockdown of NLRP3 and ASC, phosphorothioate-modified oligodeoxynucleotides (ThermoHybaid, Ulm, Germany) were used. ODN sequences complementary to corresponding mRNA sequences devoid of secondary structures, *i.e.*, loops, were selected using available algorithms.[63] The antisense ODN for ASC corresponded to nucleotides 654−676 of the human ASC mRNA (NM_145182.4) 5′-AATCCCACCAAATCATCCTGAA-3′, and, for human NLRP3, ODN corresponded to nucleotides 970−991 (NM_001079821.2) 5′-AGCTGCTGCCCCGACCCAAACC-3′. The control sequences contained the same set of base pairs in a scrambled order. The sequences were analyzed for lack of secondary structure and oligo pairing.[63] According to blast search, the selected sequences did not show any similarity to any coding mRNA. Macrophages were treated for 24 h with 5 μM ODN in RPMI 1640 supplemented with 10% FCS.[53] The cells were either lysed and analyzed for NLRP3 and ASC expression by Western immunoblotting using antibodies against NLRP3 (Epitomics) and ASC (Santa Cruz) or incubated with the nanoparticles (each 100 μg/mL) for an additional 72 h. In later experiments, the cells were supplemented with fresh ODN (5 μM) every 24 h.

Enzyme-Linked Immunosorbent Assay (ELISA). Macrophages (1×10^6 cells/mL RPMI 1640, 10% FCS) were treated with the indicated concentrations of the particles for different time periods. Cytokines (IL-1β and TNF-α) in culture supernatants were assessed with ELISA kits (R&D Systems) in accordance with the manufacturer's instructions.

Immunoprecipitation. Macrophages (5×10^6) were resuspended in 2 mL of RPMI 1640, 10% FCS, and stimulated with polystyrene nanoparticles (100 μg/mL) for 72 h. Cells were lysed with buffer containing 0.1% Nonidet P-40. Lysates were precleared with rabbit IgG and protein A-agarose beads. The NLRP3 complex or TXNIP was immunoprecipitated from the precleared cell lysates with appropriate rabbit antibodies and protein A-agarose beads. After extensive washing, the immunoprecipitated samples were separated by SDS-PAGE, blotted onto PVDF membranes, and probed for TXNIP (MBL Int.), ASC (Santa Cruz), and TXN (R&D Systems).

Redox Western Blotting. Analysis of the thioredoxin redox state was performed as described previously.[64] Macrophages were incubated with PS-NH_2 nanoparticles (100 μg/mL) for 72 h. After incubation, the cells were lysed in 6 M guanidinium chloride, 50 mM Tris pH 8.3, 3 mM EDTA, and 0.5% Triton-X-100 containing 50 mM iodoacetic acid. After 30 min incubation at 37 °C, excess iodoacetic acid was removed by Sephadex chromatography (MicroSpin G-25 columns, GE Healthcare). Protein concentrations in the eluates were determined by the Micro BCA protein assay (Thermo Scientific), and equal amounts of protein were loaded for gel separation. Eluates were separated on a native polyacrylamide gel (5% stacking gel, 15% separating gel). Gels were electroblotted to PVDF membranes and probed for thioredoxin using an antithioredoxin antibody (R&D Systems).

Molecular Modeling. Computational docking and scoring studies of the interaction of TXNIP with NLRP3 were performed using Hex 6.3[50,51] and Molegro Virtual Docker 2008.[65] The original parameters of blind docking were used in combination with an evaluation scheme based on the changes of Gibbs free energy (ΔG).[66] The 3D protein structures were generated using the I-TASSER Standalone Package (Version 1.1)[67,68] on the bases of the primary sequences of TXNIP (Q9H3M7) and NLRP3 (Q96P20) obtained from the UniProt database.

Statistical Analysis. Quantitative results are expressed as mean ± SEM. Results were analyzed by multigroup comparison Mann−Whitney U and Newman−Keuls tests. Differences were considered statistically significant at $p < 0.05$.

Acknowledgment. This work was supported by the Deutsche Forschungsgemeinschaft (DFG) through the Priority Program SPP1313 and the Center for Functional Nanostructures (CFN).

Supporting Information Available: Characterization of polystyrene nanoparticles and analysis of lysosomal permeabilization and mitochondrial ROS production. This material is available free of charge *via* the Internet at http://pubs.acs.org.

REFERENCES AND NOTES

1. Xie, J.; Huang, J.; Li, X.; Sun, S.; Chen, X. Iron Oxide Nanoparticle Platform for Biomedical Applications. *Curr. Med. Chem.* **2009**, *16*, 1278–1294.
2. Moghimi, S. M.; Hunter, A. C.; Murray, J. C. Nanomedicine: Current Status and Future Prospects. *Faseb J.* **2005**, *19*, 311–330.
3. Mora-Huertas, C. E.; Fessi, H.; Elaissari, A. Polymer-Based Nanocapsules for Drug Delivery. *Int. J. Pharm.* **2010**, *385*, 113–142.
4. Kim, S. C.; Chen, D. R.; Qi, C.; Gelein, R. M.; Finkelstein, J. N.; Elder, A.; Bentley, K.; Oberdorster, G.; Pui, D. Y. A Nanoparticle Dispersion Method for *in Vitro* and *in Vivo* Nanotoxicity Study. *Nanotoxicology* **2010**, *4*, 42–51.
5. Kim, B. Y.; Rutka, J. T.; Chan, W. C. Nanomedicine. *N. Engl. J. Med.* **2010**, *363*, 2434–2443.
6. Lunov, O.; Syrovets, T.; Rocker, C.; Tron, K.; Nienhaus, G. U.; Rasche, V.; Mailander, V.; Landfester, K.; Simmet, T. Lysosomal Degradation of the Carboxydextran Shell of Coated Superparamagnetic Iron Oxide Nanoparticles and the Fate of Professional Phagocytes. *Biomaterials* **2010**, *31*, 9015–9022.
7. Nel, A.; Xia, T.; Madler, L.; Li, N. Toxic Potential of Materials at the Nanolevel. *Science* **2006**, *311*, 622–627.
8. Xia, T.; Kovochich, M.; Liong, M.; Zink, J. I.; Nel, A. E. Cationic Polystyrene Nanosphere Toxicity Depends on Cell-Specific Endocytic and Mitochondrial Injury Pathways. *ACS Nano* **2008**, *2*, 85–96.
9. Velev, O. D.; Kaler, E. W. *In Situ* Assembly of Colloidal Particles into Miniaturized Biosensors. *Langmuir* **1999**, *15*, 3693–3698.
10. Rogach, A.; Susha, A.; Caruso, F.; Sukhorukov, G.; Kornowski, A.; Kershaw, S.; Möhwald, H.; Eychmüller, A.; Weller, H. Nano- and Microengineering: 3-D Colloidal Photonic Crystals Prepared from Sub-Mm-Sized Polystyrene Latex Spheres Pre-Coated with Luminescent Polyelectrolyte/Nanocrystal Shells. *Adv. Mater.* **2000**, *12*, 333–337.
11. Boal, A. K.; Ilhan, F.; DeRouchey, J. E.; Thurn-Albrecht, T.; Russell, T. P.; Rotello, V. M. Self-Assembly of Nanoparticles into Structured Spherical and Network Aggregates. *Nature* **2000**, *404*, 746–748.
12. Florence, A. T. Issues in Oral Nanoparticle Drug Carrier Uptake and Targeting. *J. Drug Target* **2004**, *12*, 65–70.
13. Opitz, B.; van Laak, V.; Eitel, J.; Suttorp, N. Innate Immune Recognition in Infectious and Noninfectious Diseases of the Lung. *Am. J. Respir. Crit. Care Med.* **2010**, *181*, 1294–1309.
14. Gordon, S.; Taylor, P. R. Monocyte and Macrophage Heterogeneity. *Nat. Rev. Immunol.* **2005**, *5*, 953–964.
15. Chellat, F.; Merhi, Y.; Moreau, A.; Yahia, L. Therapeutic Potential of Nanoparticulate Systems for Macrophage Targeting. *Biomaterials* **2005**, *26*, 7260–7275.
16. Amor, S.; Puentes, F.; Baker, D.; van der Valk, P. Inflammation in Neurodegenerative Diseases. *Immunology* **2010**, *129*, 154–169.
17. Swanson, J. A. Shaping Cups into Phagosomes and Macropinosomes. *Nat. Rev. Mol. Cell Biol.* **2008**, *9*, 639–649.
18. Mosser, D. M.; Edwards, J. P. Exploring the Full Spectrum of Macrophage Activation. *Nat. Rev. Immunol.* **2008**, *8*, 958–969.
19. Dostert, C.; Petrilli, V.; Van Bruggen, R.; Steele, C.; Mossman, B. T.; Tschopp, J. Innate Immune Activation through NALP3 Inflammasome Sensing of Asbestos and Silica. *Science* **2008**, *320*, 674–677.
20. Davis, B. K.; Wen, H.; Ting, J. P. The Inflammasome NLRS in Immunity, Inflammation, and Associated Diseases. *Annu. Rev. Immunol.* **2011**, *29*, 707–735.
21. Hornung, V.; Bauernfeind, F.; Halle, A.; Samstad, E. O.; Kono, H.; Rock, K. L.; Fitzgerald, K. A.; Latz, E. Silica Crystals and Aluminum Salts Activate the NALP3 Inflammasome through Phagosomal Destabilization. *Nat. Immunol.* **2008**, *9*, 847–856.
22. Martinon, F.; Mayor, A.; Tschopp, J. The Inflammasomes: Guardians of the Body. *Annu. Rev. Immunol.* **2009**, *27*, 229–265.
23. Martinon, F.; Petrilli, V.; Mayor, A.; Tardivel, A.; Tschopp, J. Gout-Associated Uric Acid Crystals Activate the NALP3 Inflammasome. *Nature* **2006**, *440*, 237–241.
24. Mariathasan, S.; Weiss, D. S.; Newton, K.; McBride, J.; O'Rourke, K.; Roose-Girma, M.; Lee, W. P.; Weinrauch, Y.; Monack, D. M.; Dixit, V. M. Cryopyrin Activates the Inflammasome in Response to Toxins and ATP. *Nature* **2006**, *440*, 228–232.
25. Halle, A.; Hornung, V.; Petzold, G. C.; Stewart, C. R.; Monks, B. G.; Reinheckel, T.; Fitzgerald, K. A.; Latz, E.; Moore, K. J.; Golenbock, D. T. The NALP3 Inflammasome Is Involved in the Innate Immune Response to Amyloid-B. *Nat. Immunol.* **2008**, *9*, 857–865.
26. Deng, Z. J.; Liang, M.; Monteiro, M.; Toth, I.; Minchin, R. F. Nanoparticle-Induced Unfolding of Fibrinogen Promotes Mac-1 Receptor Activation and Inflammation. *Nat. Nanotechnol.* **2011**, *6*, 39–44.
27. Schanen, B. C.; Karakoti, A. S.; Seal, S.; Drake, D. R., 3rd; Warren, W. L.; Self, W. T. Exposure to Titanium Dioxide Nanomaterials Provokes Inflammation of an *in Vitro* Human Immune Construct. *ACS Nano* **2009**, *3*, 2523–2532.
28. Yazdi, A. S.; Guarda, G.; Riteau, N.; Drexler, S. K.; Tardivel, A.; Couillin, I.; Tschopp, J. Nanoparticles Activate the Nlr Pyrin Domain Containing 3 (NLRP3) Inflammasome and Cause Pulmonary Inflammation through Release of IL-1α and IL-1β. *Proc. Natl. Acad. Sci. U. S. A.* **2010**, *107*, 19449–19454.
29. Winter, M.; Beer, H. D.; Hornung, V.; Kramer, U.; Schins, R. P.; Forster, I. Activation of the Inflammasome by Amorphous Silica and TiO_2 Nanoparticles in Murine Dendritic Cells. *Nanotoxicology* **2010**.
30. Morishige, T.; Yoshioka, Y.; Inakura, H.; Tanabe, A.; Yao, X.; Narimatsu, S.; Monobe, Y.; Imazawa, T.; Tsunoda, S.; Tsutsumi, Y.; *et al.* The Effect of Surface Modification of Amorphous Silica Particles on NLRP3 Inflammasome Mediated IL-1β Production, Ros Production and Endosomal Rupture. *Biomaterials* **2010**, *31*, 6833–6842.
31. Reisetter, A. C.; Stebounova, L. V.; Baltrusaitis, J.; Powers, L.; Gupta, A.; Grassian, V. H.; Monick, M. M. Induction of Inflammasome-Dependent Pyroptosis by Carbon Black Nanoparticles. *J. Biol. Chem.* **2011**, *286*, 21844–21852.
32. Lunov, O.; Syrovets, T.; Loos, C.; Beil, J.; Delacher, M.; Tron, K.; Nienhaus, G. U.; Musyanovych, A.; Mailander, V.; Landfester, K.; *et al.* Differential Uptake of Functionalized Polystyrene Nanoparticles by Human Macrophages and a Monocytic Cell Line. *ACS Nano* **2011**, *5*, 1657–1669.
33. Nemmar, A.; Hoylaerts, M. F.; Hoet, P. H.; Vermylen, J.; Nemery, B. Size Effect of Intratracheally Instilled Particles on Pulmonary Inflammation and Vascular Thrombosis. *Toxicol. Appl. Pharmacol.* **2003**, *186*, 38–45.
34. Holzapfel, V.; Musyanovych, A.; Landfester, K.; Lorenz, M. R.; Mailänder, V. Preparation of Fluorescent Carboxyl and Amino Functionalized Polystyrene Particles by Miniemulsion Polymerization as Markers for Cells. *Macromol. Chem. Phys.* **2005**, *206*, 2440–2449.
35. Musyanovych, A.; Rossmanith, R.; Tontsch, C.; Landfester, K. Effect of Hydrophilic Comonomer and Surfactant Type on the Colloidal Stability and Size Distribution of Carboxyl- and Amino-Functionalized Polystyrene Particles Prepared by Miniemulsion Polymerization. *Langmuir* **2007**, *23*, 5367–5376.
36. Waters, K. M.; Masiello, L. M.; Zangar, R. C.; Tarasevich, B. J.; Karin, N. J.; Quesenberry, R. D.; Bandyopadhyay, S.; Teeguarden, J. G.; Pounds, J. G.; Thrall, B. D. Macrophage Responses to Silica Nanoparticles Are Highly Conserved across Particle Sizes. *Toxicol. Sci.* **2009**, *107*, 553–569.
37. Xia, T.; Kovochich, M.; Brant, J.; Hotze, M.; Sempf, J.; Oberley, T.; Sioutas, C.; Yeh, J. I.; Wiesner, M. R.; Nel, A. E.

Comparison of the Abilities of Ambient and Manufactured Nanoparticles to Induce Cellular Toxicity According to an Oxidative Stress Paradigm. *Nano Lett.* **2006**, *6*, 1794–1807.
38. Nel, A. E.; Madler, L.; Velegol, D.; Xia, T.; Hoek, E. M.; Somasundaran, P.; Klaessig, F.; Castranova, V.; Thompson, M. Understanding Biophysicochemical Interactions at the Nano-Bio Interface. *Nat. Mater.* **2009**, *8*, 543–557.
39. Fujisawa, A.; Kambe, N.; Saito, M.; Nishikomori, R.; Tanizaki, H.; Kanazawa, N.; Adachi, S.; Heike, T.; Sagara, J.; Suda, T.; *et al.* Disease-Associated Mutations in Cias1 Induce Cathepsin B-Dependent Rapid Cell Death of Human THP-1 Monocytic Cells. *Blood* **2007**, *109*, 2903–2911.
40. Guicciardi, M. E.; Leist, M.; Gores, G. J. Lysosomes in Cell Death. *Oncogene* **2004**, *23*, 2881–2890.
41. Zhao, M.; Antunes, F.; Eaton, J. W.; Brunk, U. T. Lysosomal Enzymes Promote Mitochondrial Oxidant Production, Cytochrome C Release and Apoptosis. *Eur. J. Biochem.* **2003**, *270*, 3778–3786.
42. Windelborn, J. A.; Lipton, P. Lysosomal Release of Cathepsins Causes Ischemic Damage in the Rat Hippocampal Slice and Depends on NMDA-Mediated Calcium Influx, Arachidonic Acid Metabolism, and Free Radical Production. *J. Neurochem.* **2008**, *106*, 56–69.
43. Winterbourn, C. C. Reconciling the Chemistry and Biology of Reactive Oxygen Species. *Nat. Chem. Biol.* **2008**, *4*, 278–286.
44. Temkin, V.; Karin, M. From Death Receptor to Reactive Oxygen Species and C-Jun N-Terminal Protein Kinase: The Receptor-Interacting Protein 1 Odyssey. *Immunol. Rev.* **2007**, *220*, 8–21.
45. Zhou, R.; Yazdi, A. S.; Menu, P.; Tschopp, J. A Role for Mitochondria in NLRP3 Inflammasome Activation. *Nature* **2011**, *469*, 221–225.
46. Schroder, K.; Tschopp, J. The Inflammasomes. *Cell* **2010**, *140*, 821–832.
47. Zhou, R.; Tardivel, A.; Thorens, B.; Choi, I.; Tschopp, J. Thioredoxin-Interacting Protein Links Oxidative Stress to Inflammasome Activation. *Nat. Immunol.* **2010**, *11*, 136–140.
48. Nishiyama, A.; Matsui, M.; Iwata, S.; Hirota, K.; Masutani, H.; Nakamura, H.; Takagi, Y.; Sono, H.; Gon, Y.; Yodoi, J. Identification of Thioredoxin-Binding Protein-2/Vitamin D_3 up-Regulated Protein 1 as a Negative Regulator of Thioredoxin Function and Expression. *J. Biol. Chem.* **1999**, *274*, 21645–21650.
49. Holmgren, A. Thioredoxin. *Annu. Rev. Biochem.* **1985**, *54*, 237–271.
50. Ritchie, D. W.; Venkatraman, V. Ultra-Fast Fft Protein Docking on Graphics Processors. *Bioinformatics* **2010**, *26*, 2398–2405.
51. Macindoe, G.; Mavridis, L.; Venkatraman, V.; Devignes, M. D.; Ritchie, D. W. Hexserver: An FFT-Based Protein Docking Server Powered by Graphics Processors. *Nucleic Acids Res.* **2010**, *38*, W445–449.
52. Martinon, F.; Burns, K.; Tschopp, J. The Inflammasome: A Molecular Platform Triggering Activation of Inflammatory Caspases and Processing of ProIL-β. *Mol. Cell* **2002**, *10*, 417–426.
53. Laumonnier, Y.; Syrovets, T.; Burysek, L.; Simmet, T. Identification of the Annexin A2 Heterotetramer as a Receptor for the Plasmin-Induced Signaling in Human Peripheral Monocytes. *Blood* **2006**, *107*, 3342–3349.
54. Petrilli, V.; Papin, S.; Dostert, C.; Mayor, A.; Martinon, F.; Tschopp, J. Activation of the NALP3 Inflammasome Is Triggered by Low Intracellular Potassium Concentration. *Cell Death Differ.* **2007**, *14*, 1583–1589.
55. Marina-Garcia, N.; Franchi, L.; Kim, Y. G.; Miller, D.; McDonald, C.; Boons, G. J.; Nunez, G. Pannexin-1-Mediated Intracellular Delivery of Muramyl Dipeptide Induces Caspase-1 Activation *Via* Cryopyrin/NLRP3 Independently of Nod2. *J. Immunol.* **2008**, *180*, 4050–4057.
56. Dostert, C.; Guarda, G.; Romero, J. F.; Menu, P.; Gross, O.; Tardivel, A.; Suva, M. L.; Stehle, J. C.; Kopf, M.; Stamenkovic, I.; *et al.* Malarial Hemozoin Is a NALP3 Inflammasome Activating Danger Signal. *PLoS One* **2009**, *4*, e6510.
57. Pelegrin, P.; Surprenant, A. Dynamics of Macrophage Polarization Reveal New Mechanism to Inhibit IL-1β Release through Pyrophosphates. *EMBO J.* **2009**, *28*, 2114–2127.
58. Colognato, R.; Slupsky, J. R.; Jendrach, M.; Burysek, L.; Syrovets, T.; Simmet, T. Differential Expression and Regulation of Protease-Activated Receptors in Human Peripheral Monocytes and Monocyte-Derived Antigen-Presenting Cells. *Blood* **2003**, *102*, 2645–2652.
59. Jiang, X.; Weise, S.; Hafner, M.; Rocker, C.; Zhang, F.; Parak, W. J.; Nienhaus, G. U. Quantitative Analysis of the Protein Corona on FePt Nanoparticles Formed by Transferrin Binding. *J. R. Soc. Interface* **2010**, *7* (Suppl. 1), S5–S13.
60. Jiang, X.; Rocker, C.; Hafner, M.; Brandholt, S.; Dorlich, R. M.; Nienhaus, G. U. Endo- and Exocytosis of Zwitterionic Quantum Dot Nanoparticles by Live Hela Cells. *ACS Nano* **2010**, *4*, 6787–6797.
61. Syrovets, T.; Jendrach, M.; Rohwedder, A.; Schüle, A.; Simmet, T. Plasmin-Induced Expression of Cytokines and Tissue Factor in Human Monocytes Involves AP-1 and IKKβ-Mediated NF-κB Activation. *Blood* **2001**, *97*, 3941–3950.
62. Burysek, L.; Syrovets, T.; Simmet, T. The Serine Protease Plasmin Triggers Expression of MCP-1 and CD40 in Human Primary Monocytes *Via* Activation of P38 MAPK and Janus Kinase (Jak)/Stat Signaling Pathways. *J. Biol. Chem.* **2002**, *277*, 33509–33517.
63. Zuker, M. Mfold Web Server for Nucleic Acid Folding and Hybridization Prediction. *Nucleic Acids Res.* **2003**, *31*, 3406–3415.
64. Watson, W. H.; Pohl, J.; Montfort, W. R.; Stuchlik, O.; Reed, M. S.; Powis, G.; Jones, D. P. Redox Potential of Human Thioredoxin 1 and Identification of a Second Dithiol/Disulfide Motif. *J. Biol. Chem.* **2003**, *278*, 33408–33415.
65. Thomsen, R.; Christensen, M. H. Moldock A: New Technique for High-Accuracy Molecular Docking. *J. Med. Chem.* **2006**, *49*, 3315–3321.
66. Hetenyi, C.; van der Spoel, D. Efficient Docking of Peptides to Proteins without Prior Knowledge of the Binding Site. *Protein Sci.* **2002**, *11*, 1729–1737.
67. Roy, A.; Kucukural, A.; Zhang, Y. I-Tasser: A Unified Platform for Automated Protein Structure and Function Prediction. *Nat. Protoc.* **2010**, *5*, 725–738.
68. Zhang, Y. Template-Based Modeling and Free Modeling by I-Tasser in Casp7. *Proteins* **2007**, *69* (Suppl. 8), 108–117.